Chemistry & Biology, Vol. 10, 397–410, May, 2003, ©2003 Elsevier Science Ltd. All rights reserved. DOI 10.1016/S1074-5521(03)00093-0

Chemical Genetic Modifier Screens: Small Molecule Trichostatin Suppressors as Probes of Intracellular Histone and Tubulin Acetylation

Kathryn M. Koeller,[1,3] Stephen J. Haggarty,[1,2,3] Brian D. Perkins,[2] Igor Leykin,[5] Jason C. Wong,[1,3] Ming-Chih J. Kao,[5] and Stuart L. Schreiber[1,2,3,4,6]

[1]Department of Chemistry and Chemical Biology
[2]Department of Molecular and Cellular Biology
[3]Harvard Institute of Chemistry and Chemical Biology
[4]Howard Hughes Medical Institute
Harvard University
12 Oxford Street
Cambridge, Massachusetts 02138
[5]Department of Biostatistics
Harvard School of Public Health
655 Huntington Avenue
Boston, Massachusetts 02115

Summary

Histone deacetylase (HDAC) inhibitors are being developed as new clinical agents in cancer therapy, in part because they interrupt cell cycle progression in transformed cell lines. To examine cell cycle arrest induced by HDAC inhibitor trichostatin A (TSA), a cytoblot cell-based screen was used to identify small molecule suppressors of this process. TSA suppressors (ITSAs) counteract TSA-induced cell cycle arrest, histone acetylation, and transcriptional activation. Hydroxamic acid-based HDAC inhibitors like TSA and suberoylanilide hydroxamic acid (SAHA) promote acetylation of cytoplasmic α-tubulin as well as histones, a modification also suppressed by ITSAs. Although tubulin acetylation appears irrelevant to cell cycle progression and transcription, it may play a role in other cellular processes. Small molecule suppressors such as the ITSAs, available from chemical genetic suppressor screens, may prove to be valuable probes of many biological processes.

Introduction

Histone acetylation is tightly coordinated with transcriptional regulation, differentiation, and cell cycle progression in mammalian cell lines (Figure 1) [1]. Aberrant histone acetylation patterns can alter differentiation pathways or disrupt cell cycle checkpoints relevant to the onset or maintenance of cancerous states. Enzymes regulating histone modifications therefore represent attractive chemotherapeutic targets. In particular, histone deacetylase (HDAC) inhibitors induce differentiation, cell cycle arrest, or apoptosis in transformed cell lines, processes most likely involving transcriptional activation [2]. For example, HDAC inhibitors and retinoic acid act synergistically to reactivate silenced genes in "differentiation therapy" for acute promyelocytic leukemia [3]. The potential of HDAC inhibitors in the treatment of T cell lymphoma [4] and neurodegenerative diseases [5] is also being explored in clinical trials of HDAC inhibitors like suberoylanilide hydroxamic acid (SAHA) [2]. Other small molecules known to inhibit HDACs (i.e., butyrate, valproic acid) already enjoy widespread clinical acceptance in the treatment of other disorders [6]. Based on these encouraging early clinical outcomes, numerous programs have been established for the discovery of potent and potentially paralog-selective HDAC inhibitors [7].

Histone acetylation is controlled by HDACs, histone acetyltransferases (HATs), and the proteins that position these enzymes to chromatin sites within the genome. HDAC inhibitors shift a reversible histone acetylation/deacetylation state (mediated by HATs and HDACs, respectively) toward a condition of histone hyperacetylation (Figure 1). HDAC inhibitors trichostatin A (TSA) and SAHA promote acetylation of α-tubulin as well as histones, implying that tubulin acetylation is also controlled by competition between acetyltransferases and deacetylases. Interestingly, not all HDAC inhibitors affect tubulin acetylation, indicating that distinguishing features exist for each class of these small molecules. Functionally, HDAC inhibitor-promoted histone acetylation correlates with cell cycle arrest and transcriptional activation. However, cellular effects of HDAC inhibitor-induced tubulin acetylation remain largely uncharacterized. As such, tubulin acetylation represents a variable that has not been recognized in cellular and clinical analysis of HDAC inhibitors like SAHA. To probe further the cellular activities of TSA, a chemical genetic modifier screen was undertaken, specifically aimed at the discovery of small molecule TSA suppressors. This strategy has identified new probes of intracellular acetylation, the cell cycle, and acetylation-mediated transcriptional activation in mammalian cell lines.

Results and Discussion

Cell-Based Screening Identifies Suppressors of TSA-Induced Cell Cycle Arrest

In classical genetics, a specific cellular phenotype is often characterized by identifying conditions or mutations that modify (i.e., suppress or enhance) the phenotype. By analogy to classical genetics, the cellular action of a chemical (here the HDAC inhibitor TSA) can be studied by identifying new small molecules that modify its cellular effects. In this respect, a chemical genetic modifier screen was used to identify small molecules that suppress TSA's cell cycle effects. TSA [8] inhibits all known class I and II HDACs in vitro and causes transcriptional activation and cell cycle arrest in mammalian cell lines. Small molecule TSA suppressors (ITSAs, *i*nhibitors of *TSA*) may thus affect components up- or downstream of HDAC inhibition.

A cytoblot modifier screen in human A549 lung carcinoma cells was used to identify ITSAs (Figure 2A) [9].

[6]Correspondence: sls@slsiris.harvard.edu

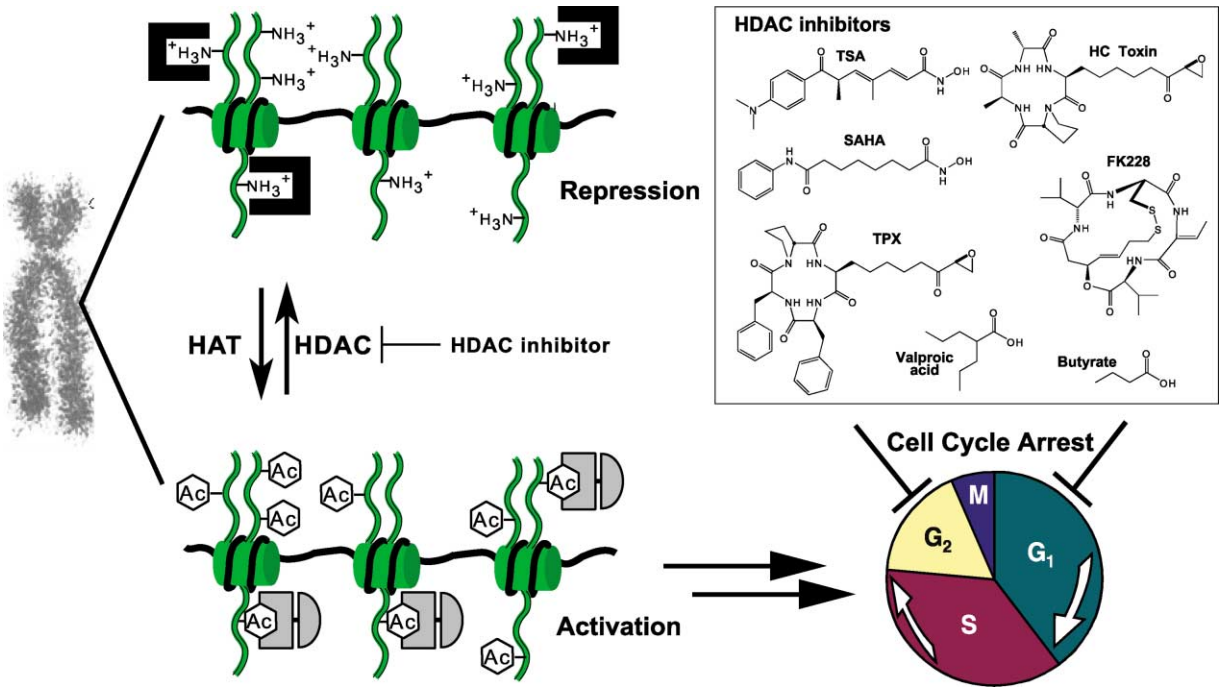

Figure 1. Regulation of Transcription and Cell Cycle Progression by HDACs and HATs

HDAC inhibitors lead to histone hyperacetylation and G1 or G2 cell cycle arrest in mammalian cells.

Briefly, this strategy involved arresting cells in the G1 and G2 phases of the cell cycle (with TSA), incubating these cells with a random library of small molecules, and detecting those small molecules that allowed cells to overcome the cell cycle blockade (ITSAs). For detection purposes, cells able to bypass arrest in G1 or G2 were captured in mitosis by nocodazole, a small molecule that destabilizes the microtubule cytoskeleton, resulting in mitotic spindle defects and cell cycle arrest in M phase. Measuring an increase in phosphonucleolin (a protein modification state specific to mitotic arrest, as well as the epitope recognized by the TG-3 antibody) then provided a means to identify the ITSAs. After two rounds of screening, 23 ITSAs were identified from 9600 small molecules (Figure 2B). Certain ITSA core structures appeared multiple times (ITSA1 and analogs), and two ITSAs (Figure 2B, asterisks) had "hit" previously in an antimitotic screen [10]. ITSAs showing assay overlap (asterisks), poor solubility, or high toxicity (ITSA2) were not pursued further. Benzotriazole-based suppressor ITSA1 exhibited adequate solubility and potency and was the main focus of further study.

Additional cellular assays confirmed that ITSAs suppress TSA's antiproliferative effects. ITSAs were first evaluated in a bromo-deoxyuridine (BrdU) cytoblot assay to assess progression though S phase of the cell cycle (Figure 2C). In murine embryonic stem (ES) cells, TSA treatment (23 hr) inhibited BrdU incorporation versus the control (no TSA). TSA-pretreated cells incubated with ITSA1, ITSA3, or ITSA4 (50 μM), however, incorporated BrdU at concentrations where it was inhibited by TSA alone. Fluorescence-activated cell sorting (FACS) analysis was then undertaken in A549 cells (Figure 2D). In TSA-treated cells (300 nM, 22 hr), 43% of the total population was apoptotic, while this number was decreased to 1% in TSA-treated cells that also received ITSA1 (50 μM, 5 hr). In actively cycling cells, TSA treatment caused a buildup in G0-G1 (41%) and G2-M (55%), while S phase was depleted (4%). Again, ITSA1 treatment served to revert the TSA-arrested population to a normal cell cycle distribution. Finally, ITSAs were also able to effect cell cycle rescue over longer duration. Murine FM3A cells [8] arrested and remained constant in number throughout several days of TSA treatment (80 nM) (see Figure 4B). Simultaneous TSA (80 nM) and ITSA (50 μM) treatment resulted in proliferation (although not to the same extent as in untreated cells), consistent with the ability of these small molecules to balance each other's activity. Collectively, these experiments establish ITSAs as probes capable of counteracting TSA-induced cell cycle arrest.

ITSAs Suppress TSA-Induced Histone Acetylation

TSA and structural analog SAHA [11] induce histone hyperacetylation in a number of mammalian cell lines. TSA (300 nM) treatment of A549 cells (2 hr) noticeably increased levels of acetyl-histone H3 (Figure 3A), while subsequent incubation with ITSA1, ITSA3, ITSA4, or ITSA5 (50 μM, 2 hr) reduced histone acetylation to the baseline level. Negative control ITSA1 analogs (nITSA1-A and -B) exhibited little or no suppressor activity. In murine ES cells, ITSA1 activity was more dramatic, fully suppressing TSA-induced acetylation within 30 min (Figure 3B). Within this rapid time course, levels of cell cycle regulatory proteins p21, cyclins, and cyclin dependent kinases (CDKs), as well as HDAC1 and histone H1 (data not shown) were unaltered. Induction of CDK inhibitor p21 is often cited as underlying cell cycle arrest due to

HDAC inhibitors [12]. However, in murine ES cells the basal p21 level was significant and insensitive to TSA.

Importantly, suppression of acetylation levels was only observable when ITSA1 was added concurrent with or post TSA treatment. Cells pretreated with ITSA1 before addition of TSA exhibited elevated acetylation levels characteristic of TSA treatment alone (data not shown). This suggests that the target of ITSA1 is not present (or, alternatively, not correctly localized) until induced by TSA. Possible targets include enzymes and complexes recruited to or associated with acetylated histone tails. In this sense, chromatin remodeling complexes, bromodomain-containing proteins, and HATs all represent potential ITSA1 targets, as do components of signaling cascades that lead to their recruitment [13]. Because TSA pretreatment is necessary for suppression by ITSA1, the possibility that ITSA1 inactivates TSA though chemical acylation was entertained. Acylation of TSA's hydroxamic acid group would inactivate the functionality required for HDAC inhibition, thus "suppressing" TSA's activity. To test this hypothesis, total in vitro HDAC activity of a HeLa cell lysate was measured in the presence of TSA, ITSA1, or TSA + ITSA1 (Figure 3C). ITSA1 alone (50 or 100 μM) had no effect on HDAC activity, making it unlikely that ITSA1 affects HDAC function directly. As expected, TSA (500 nM) partially inhibited HDAC activity of the total lysate. Notably, the level of inhibition for simultaneous treatment with TSA (500 nM) and ITSA1 (50 or 100 μM) was nearly identical to that of TSA alone, suggesting that TSA and ITSA1 do not directly interact, chemically or otherwise. To determine whether ITSA1 could possibly be acylating HATs or histone proteins, thereby destroying the acetylating enzyme or substrate, cellular wash-out experiments were undertaken. A549 cells were treated with TSA (300 nM, 2 hr) followed by ITSA1 (50 μM, 2 hr). Cellular media was then removed and replaced with media containing TSA alone (300 nM) for various time periods. Even at the shortest wash-out time point examined (30 min), TSA-induced acetylation of histones and tubulin was readily observable (data not shown). As such, ITSA1 does not likely covalently modify histones or HATs.

Trapoxin B (TPX) [14] and HC Toxin (both epoxyketones) and FK228 [15] (a depsipeptide originally named FR901228) are potent HDAC inhibitors structurally distinct from hydroxamates TSA and SAHA. Collectively, these small molecules encompass various known classes of HDAC inhibitors all thought to act by similar mechanisms, with at least some functional redundancy (in vitro). While TSA and SAHA inhibit all class I and II HDACs in vitro, inhibitors like TPX inhibit all but HDAC6 [16] (and the recently identified, sequence-related HDAC10 [17]). Analysis of bulk histone acetylation levels alone does not indicate differences in the activities of these HDAC inhibitors in cells, as all induce histone acetylation (Figure 3D). However, ITSA1 possesses differential suppressor activity toward the different classes and can be used to distinguish them. In this respect, ITSA1 (50 μM) suppressed histone acetylation induced by TSA (300 nM) and SAHA (3 μM) but not by TPX (50 nM), HC Toxin (50 nM), or FK228 (10 nM). The inability of ITSA1 to suppress FK228 further suggests that ITSA1 does not nonspecifically acylate thiol groups, the nucleophilic functionality of this HDAC inhibitor [18]. Notably, cell cycle arrest induced by HC Toxin was also insensitive to ITSA1 (Figure 2D). This intriguing ability of ITSA1 to differentially suppress TSA-like versus TPX-like molecules may reflect targeting of these HDAC inhibitors to different multisubunit complexes with varying degrees of accessibility, rather than inhibition of specific HDAC orthologs. Indeed, the sets of genes upregulated in TSA- versus TPX-treated cells (see Profiling section below) were observed to be nonoverlapping and associated with different promoter elements, suggesting alternative targeting.

Several but Not All ITSAs Suppress TSA-Induced Tubulin Acetylation

TSA and SAHA induce acetylation of cytoplasmic α-tubulin at lysine-40. TSA treatment reversibly transforms "short and curly" acetylated microtubules concentrated around the centrosome and Golgi apparatus into an "extended and straight" acetylated microtubule population throughout the entire cell body (Figure 4A). This effect of TSA was observable in less than 2 hr in A549 or murine ES cells (Figures 3A and 3B). Subsequent ITSA1 or ITSA3 treatment (50 μM) suppressed tubulin acetylation (30 min–2 hr), while nITSA1-A and -B (50 μM) were ineffective (Figure 3A). Interestingly, ITSA4 and ITSA5 (50 μM) also failed to suppress tubulin acetylation, indicating that multiple categories of suppressors exist within the ITSA population. Since only a few ITSAs suppress tubulin acetylation, this property is not required to bypass TSA-induced cell cycle arrest, the main condition of the original screen. Furthermore, in TSA-resistant cell line TR303 [8], proliferation was normal in the presence of TSA (80 nM). While TR303 cells were not subject to histone hyperacetylation by TSA, tubulin acetylation was augmented in both FM3A (TSA-sensitive) and TR303 cells (Figure 4B).

Tubulin acetylation is often associated with factors that increase cytoskeletal stability, such as the microtubule-stabilizing agent taxol [19]. The possibility that TSA causes an increase in α-tubulin acetylation by stabilizing the microtubule cytoskeleton was therefore investigated. A549 cells were pretreated (2 hr) with either taxol (10 μM) or TSA (300 nM) followed by the addition of ITSA1 (50 μM, 1 hr). Interestingly, ITSA1 decreased tubulin acetylation caused by TSA (Figure 4C) but not taxol (Figures 4C and 4D). Global acetylation phenotypes induced by TSA and taxol were also morphologically distinct. Whereas taxol caused visible clumping and bundling of microtubules, TSA-treated cells lacked visible microtubule abnormalities (Figure 4C). A common mechanism of action for these agents is therefore unlikely. TSA may instead augment tubulin acetylation by directly inhibiting a tubulin deacetylase (TDAC), such as HDAC6 [20]. The ability of ITSA1 to differentially suppress TSA-induced but not taxol-induced tubulin acetylation was exploited to screen and characterize a library of new acetylation-inducing small molecules (see accompanying manuscript [21]). In this screen, ITSA1 suppressed $\sim$70% (338 of 475) of the newly discovered tubulin acetylation-inducing hydroxamic acids (TSA-like), while having no effect on the remaining $\sim$30%

A

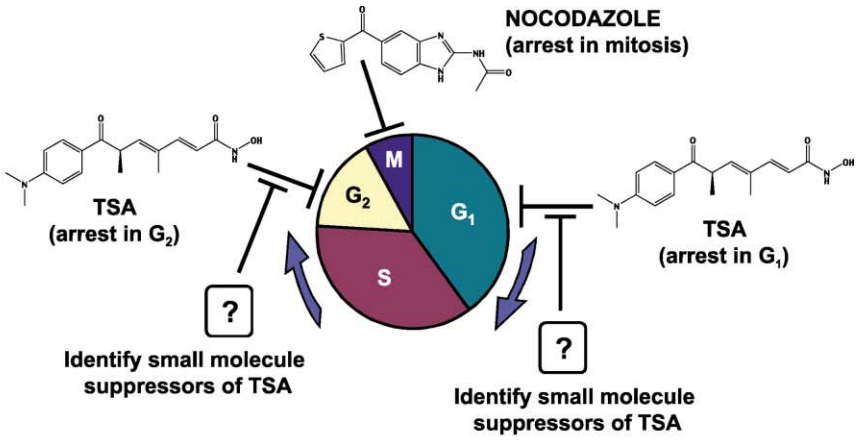

B

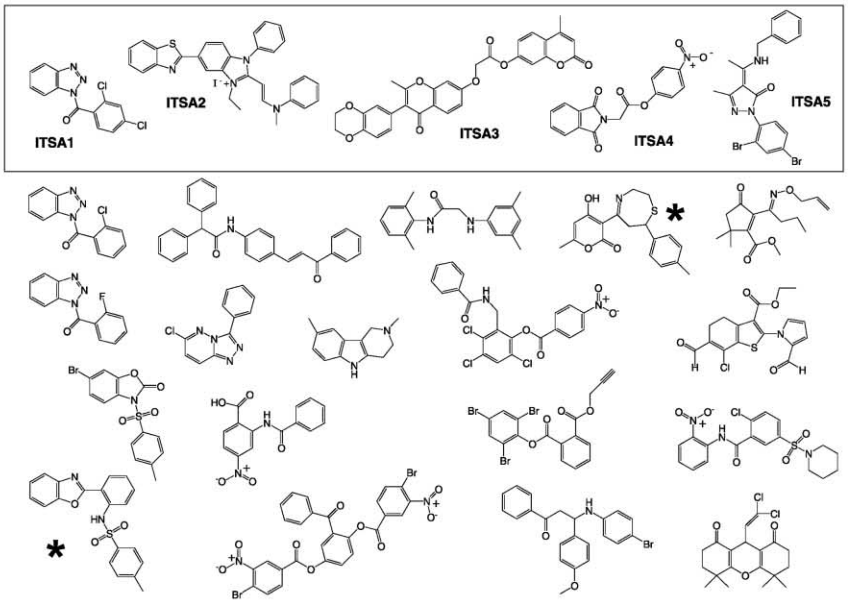

C

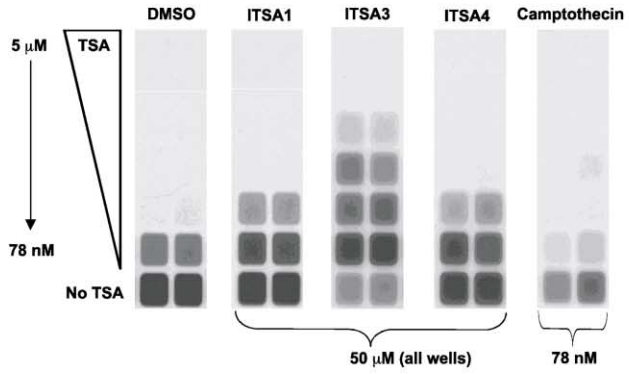

D

	Cell Cycle Analysis (%)				Apoptotic Analysis (%)
	G_0-G_1	S	G_2-M	Total	< 2n
DMSO	26	48	26	100	2
DMSO + ITSA1	37	51	12	100	6
TSA	41	4	55	100	43
TSA + ITSA1	58	32	10	100	1
HC Toxin	32	0	68	100	38
HC Toxin + ITSA1	31	0	69	100	52

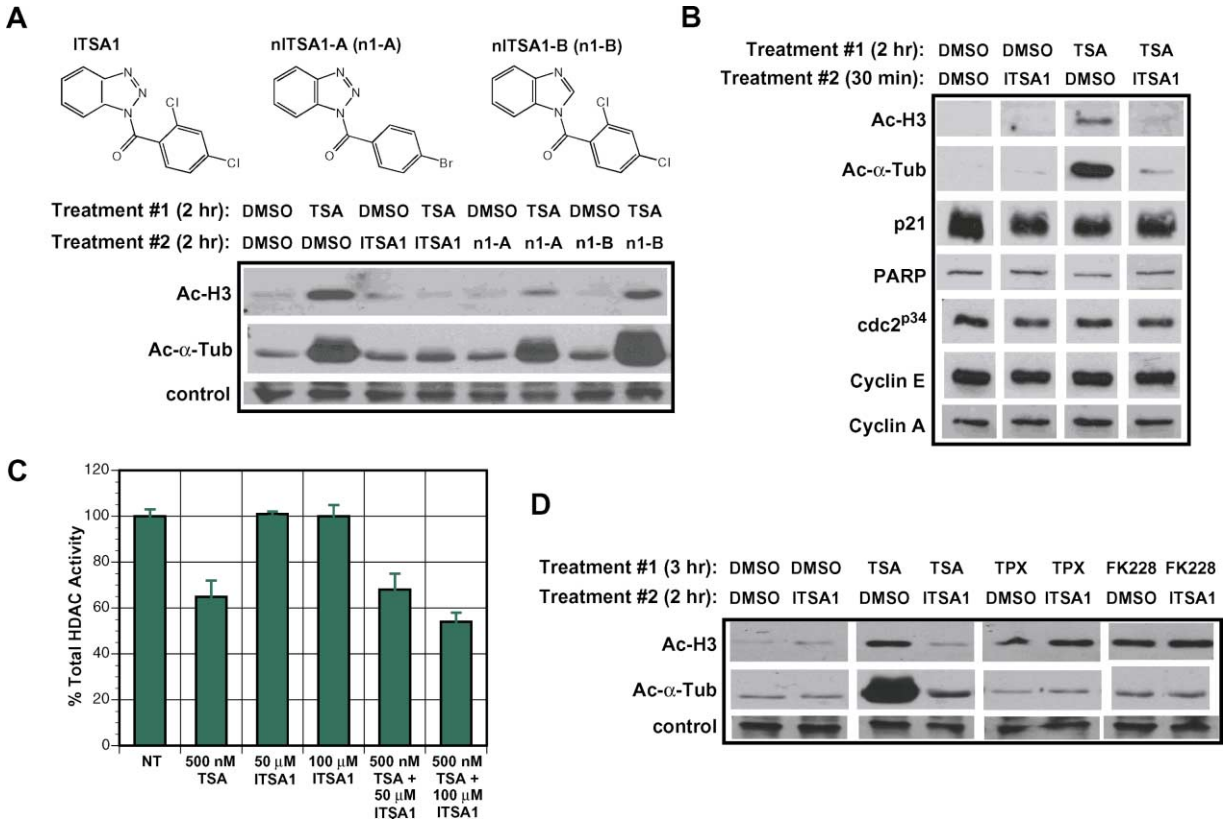

Figure 3. Suppression of TSA-Induced Histone and Tubulin Acetylation by ITSA1

(A) ITSA1 (50 μM) suppresses TSA-induced (300 nM) histone and tubulin acetylation in A549 cells, while negative control analogs (50 μM) do not.

(B) ITSA1 (50 μM) suppresses acetylation induced by TSA (300 nM) without affecting levels of other cell cycle regulatory proteins in murine ES cells.

(C) In vitro HDAC assay using total HeLa cell lysate as the source of enzymatic activity. ITSA1 does not affect HDAC activity in the presence or absence of TSA.

(D) TPX (50 nM) and FK228 (10 nM) induce histone acetylation but not tubulin acetylation in A549 cells. ITSA1 (50 μM) does not suppress histone acetylation due to TPX or FK228.

(taxol-like). These results further detract from an ITSA1 acylation mechanism, as ITSA1 does not appear to react nonspecifically with all hydroxamates in this small molecule library.

Unlike TSA (Figures 3 and 4) and SAHA (Figure 4E), epoxy-ketone-based HDAC inhibitors TPX and HC Toxin do not induce α-tubulin acetylation (Figure 3C), yet potently impede cell cycle progression (Figure 2D). As such, tubulin acetylation induced by TSA does not appear related to its cell cycle arresting activity. In turn, TPX-like compounds may be more specific HDAC inhibitors than TSA or SAHA, targeting nuclear deacetylases selectively. Absence of an effect on tubulin acetylation coupled with the insensitivity of HDAC6 to TPX supports the idea that HDAC6 is a tubulin deacetylase. The ability to segregate HDAC from TDAC inhibition in analyzing TSA-induced cell cycle arrest would be aided by a TDAC selective inhibitor. Marginally "selective" HDAC inhibitors like TPX are useful but still have the caveat of inhibiting multiple HDACs nonselectively. A small molecule inducer of tubulin acetylation has recently been discovered though cytoblot screening [21] of an "HDAC-biased" library [22]. Tubacin (*tub*ulin *ac*etylation *in*ducer) was found to specifically induce tubulin acetylation and

Figure 2. Identification of ITSAs through Cell-Based Screening

(A) TG-3 cytoblot TSA suppressor screen in A549 cells. Nocodazole is used to capture cells released from a TSA-induced G1 or G2 cell cycle block by an ITSA. After two rounds of screening, 23 ITSAs (out of a 9600 member library) were active at a level of 2-fold or greater versus controls (DMSO alone).

(B) Molecular structures of ITSAs in the Chembridge library.

(C) Cell-based BrdU incorporation assay in murine ES cells. TSA inhibits BrdU incorporation (>78 nM), while ITSAs (50 μM) allow BrdU incorporation in the presence of TSA.

(D) FACS analysis of HDAC inhibitors in A549 cells ([TSA] = 500 nM, [HC Toxin] = 500 nM) in the presence and absence of ITSA1 (50 μM): (1) cell cycle distribution in cycling cells and (2) apoptosis in the total cellular population.

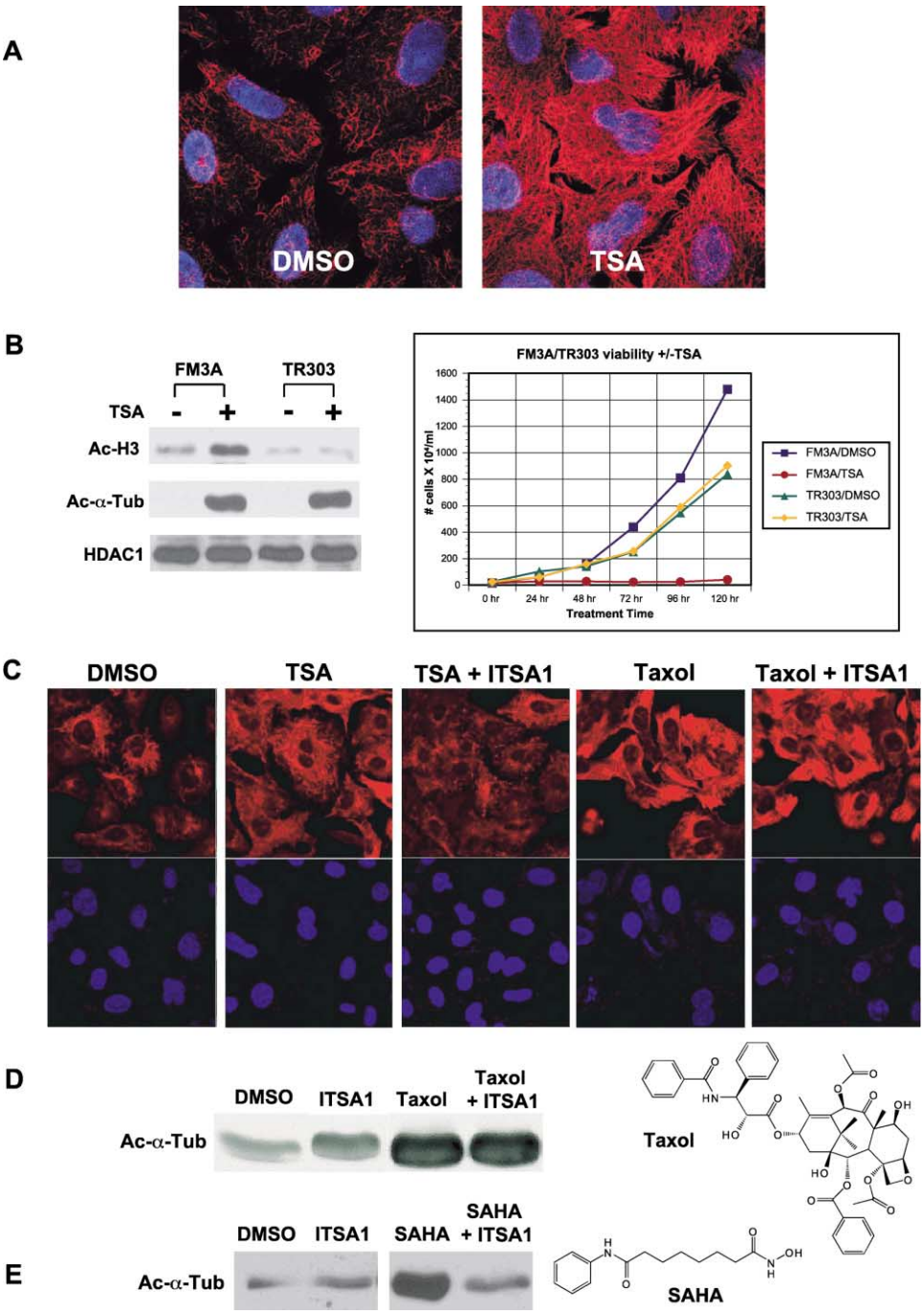

Figure 4. Tubulin Acetylation Phenotypes Induced by TSA, Taxol, and SAHA

(A) TSA-induced (2 μM) tubulin acetylation in A549 cells.

(B) TSA-resistant TR303 cells are viable in the presence of TSA (80 nM) and exhibit tubulin acetylation but not histone acetylation. Isogenic TSA-sensitive FM3A cells exhibit TSA-induced (80 nM) histone and tubulin acetylation as well as cell cycle arrest.

(C) Cellular tubulin acetylation phenotypes induced by TSA (300 nM) and taxol (10 μM) are morphologically distinct in A549 cells. ITSA1 (50 μM) suppresses effects of TSA but not taxol on the cytoskeleton.

(D) ITSA1 (50 μM) does not suppress taxol-induced (10 μM) tubulin acetylation in A549 cells.

(E) ITSA1 (50 μM) suppresses tubulin acetylation induced by SAHA (300 nM) in A549 cells.

inhibit HDAC6 in vitro without affecting histone acetylation or the cell cycle [23]. TSA and tubacin induce morphologically similar microtubule phenotypes and are both suppressible by ITSA1, implying that tubacin has the tubulin acetylation-augmenting component of TSA's activity. This molecule has proven useful in dissecting cellular consequences of tubulin acetylation away from histone acetylation.

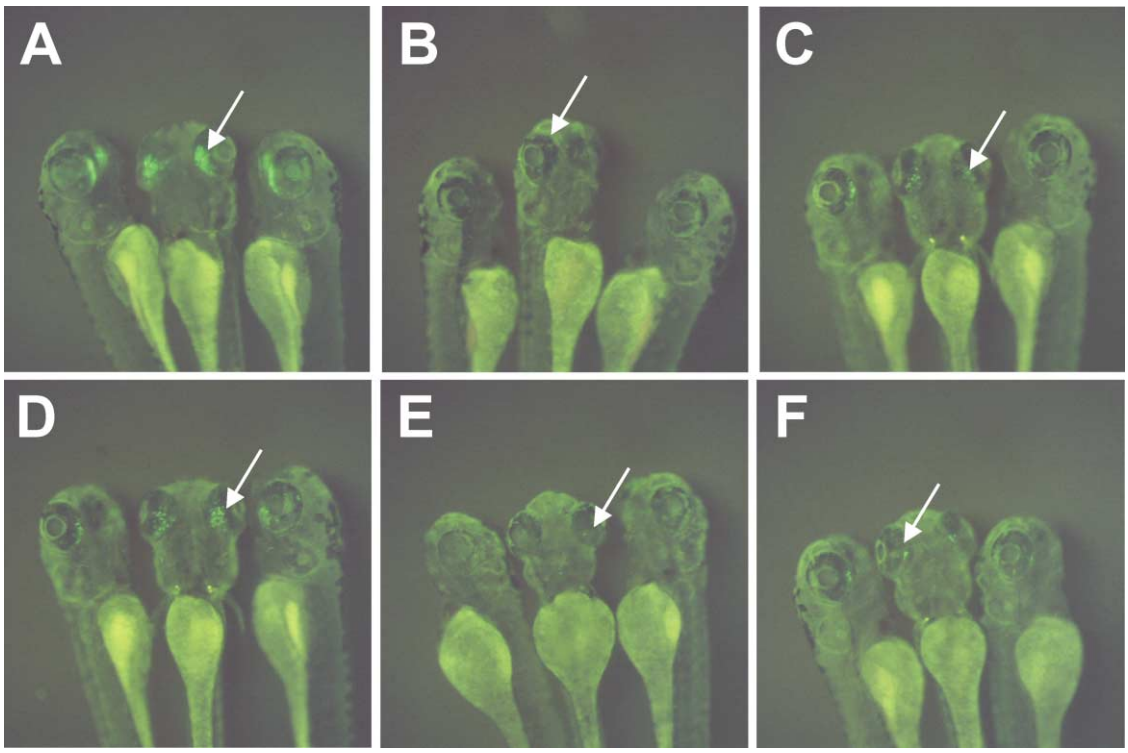

Figure 5. ITSA1 Reactivates Transcription from a TSA-Repressed Rhodopsin-GFP Transgene in Zebrafish Eye

(A), DMSO control; (B), 3 mM valproic acid; (C), 300 nM TSA; (D), 300 nM TSA + 30 μM ITSA1; (E), 300 nM TSA + 30 μM nITSA1-A; (F), 300 nM TSA + 30 μM nITSA1-B.

ITSAs Suppress TSA-Induced Phenotypes in the Zebrafish Eye

ITSAs provide numerous avenues of study in mammalian cell lines, but the ability to use these small molecules in living organisms would further broaden their scope. Chemical genetic screens in zebrafish have previously identified small molecules that induce striking phenotypes [24]. For example, retinoic acid has been used to study development of the vertebrate eye [25]. Treating zebrafish with retinoic acid during critical periods of retinal development results in precocious development of rod photoreceptors. Given the similar and oftentimes synergistic roles of TSA and retinoic acid in stimulating transcription [3], the effect of TSA on retinal development in the zebrafish was examined.

A transgenic line of zebrafish expressing a green fluorescent protein (GFP)-rhodopsin C-terminal fusion protein under control of a rod photoreceptor cell-specific promoter (opsin) was selected for analysis [26]. GFP-transgene expression was readily visible in rods present in the ventral retina (Figure 5A), and this expression pattern expanded upon treatment with retinoic acid [26]. When these fish were treated with 3 mM valproic acid (Figure 5B) or 300 nM TSA (Figure 5C), GFP expression was eliminated or significantly reduced. No other physiological processes, such as heart rate or swimming ability, were noticeably affected. This result is surprising, as GFP expression was expected to *increase* upon treatment with HDAC inhibitors. The possibility that HDACs may activate transcription [27] of the rhodopsin gene must be considered in explaining this outcome. Alternatively, the GFP-rhodopsin transgene may be inserted in a chromatin region unlike the endogenous context, rendering the transgene directly or indirectly silenced by HDAC inhibition. In such a scenario, accessibility of specific chromatin-modifying complexes may be the dominating factor in transcriptional regulation. Notably, TSA-induced loss of GFP was rescued by addition of 30 μM ITSA1 (Figure 5D) or ITSA3 but not ITSA4. Suppression of TSA by ITSA1 was highly specific, as negative controls nITSA1-A and -B (30 μM) were inactive (Figures 5E and 5F). Collectively, these results suggest the expression of the GFP-rhodopsin transgene is regulated though a mechanism involving reversible acetylation of histones. TSA and ITSAs provide new tools to modulate and control these processes in a living vertebrate organism.

Transcriptional Profiling with HDAC Inhibitors and ITSA1

Profiling experiments were undertaken to examine transcripts regulated by TSA and ITSA1 and to assess differences between the various classes of HDAC inhibitors. Profiles were obtained in murine ES cells, as TSA-induced acetylation was dramatic and rapid in this cell line, and HDAC inhibitor profiling [27, 28] has not been reported in ES cells. Reasoning that the shortest possible treatment time would reduce secondary or nonspecific transcriptional effects, the minimum treatment duration required for TSA-induced histone acetylation (300 nM, 2 hr) and subsequent ITSA1 suppression (50 μM, 30 min) was determined (Figure 3B). The ability of TPX

to induce histone acetylation (50 nM, 2 hr), and tubacin to promote tubulin acetylation (2 μM, 2 hr) under these conditions was also confirmed. Data sets were obtained in duplicate by treating murine ES cells with the following small molecule combinations (treatment 1 [2 hr]/treatment 2 [30 min]): (1) DMSO/DMSO, (2) TSA/DMSO, (3) TPX/DMSO, (4) tubacin/DMSO, (5) DMSO/ITSA1, and (6) TSA/ITSA1. Samples were processed following Affymetrix protocols, and data sets were analyzed with dCHIP1.0 software [29] (see Supplemental Data at http://www.chembiol.com/cgi/content/full/10/5/397/DC1 or write to chembiol@cell.com for a PDF). When considering genes highly upregulated by TSA, TPX, or ITSA1, reproducibility between the duplicates was high. Although suppression was observed in both TSA/ITSA1 (profile 6) data sets, one sample exhibited complete suppression, while the other was only partially suppressed. Expression values for all duplicate data sets were pooled by a weighted averaging method. Fold-change levels represent the lower statistical bound of the actual measured fold-change versus control DMSO profile (1).

TSA profile (2) exhibited robust transcriptional activation (Figure 6A). Above a 2-fold cut-off, 133 of 139 genes present in TSA profile (2) were upregulated. Notably, ITSA1 treatment abrogated expression of this highly activated transcript population (Figure 6B), further correlating TSA-induced cell cycle arrest and histone acetylation with transcriptional activation. ITSA1 profile (5) showed only low-level transcriptional activation and repression (Figure 6C). Compared to the suppression activity of ITSA1 observed following TSA treatment, this result again suggests the target of ITSA1 is induced following TSA treatment. Genes downregulated in TSA profile (2) were only marginally decreased (<1.5-fold), implying that negative transcripts represent indirect results of TSA treatment or a secondary cellular response.

TPX profile (3) contained a number of upregulated transcripts (Figure 6D) but at a level appreciably dampened versus TSA profile (2). Altered kinetics in the action of TSA and TPX may explain this result, as experiments were optimized for TSA-induced acetylation levels. In TPX profile (3), several genes were highly upregulated (>2-fold) and likely represent specific transcriptional targets of TPX. Although the magnitude of ITSA1 profile (5) and TPX profile (3) appear similar (Figures 6C and 6D), ITSA1 profile (5) lacks a highly activated gene population (>2-fold). Tubacin profile (4) was generally absent of transcriptional activity, further segregating tubulin acetylation from TSA's effects on the cell cycle or transcription. Tubacin therefore has great utility in the analysis of tubulin acetylation induced by HDAC inhibitors, in a fashion uncoupled from histone acetylation [23].

Transcripts Upregulated by HDAC Inhibitors TSA and TPX Differ

Several transcripts activated in TSA profile (2) are consistent with prior reports of HDAC-regulated genes (Figure 6E). For example, the prolactin promoter is derepressed by TSA though inhibition of HDACs in the NCoR/mSin3A complex [30], and TSA is known to induce expression of the lysozyme M gene [31]. Other TSA-upregulated genes are related to histones and cell cycle proteins, such as granzyme A, a protease known to degrade histones and mediate cell death [32]. Interestingly, expression of these TSA-induced genes was suppressed by ITSA1. When compared to profiles of murine stem cells in various stages of differentiation, TSA profile (2) includes genes not generally used by these cells at any stage of their developmental program [33]. In TSA profile (2), the absence of general cell cycle regulatory proteins often cited in the context of HDAC inhibitor-induced arrest is noteworthy. This may reflect nonspecific activity of TSA toward various deacetylases, metalloproteases, and other proteins [34]. Surprisingly, TPX profile (3) was essentially nonoverlapping with TSA profile (2), suggesting these HDAC inhibitors act though distinct mechanisms to regulate gene expression. This result may underlie the ability of ITSA1 to suppress cellular functions of TSA but not TPX. TPX-activated transcripts included those typically cited as responsive to HDAC inhibitors, including cell cycle regulatory proteins like p21 and Jund1. Mapping TSA- and TPX-upregulated genes to their respective chromosomal locations revealed distinct patterns for each of these HDAC inhibitors (Figure 6F), possibly illustrating unique targeting patterns of these molecules (see Supplemental Data at http://www.chembiol.com/cgi/content/full/10/5/397/DC1 or write to chembiol@cell.com for a PDF).

Promoter Region Analysis

Analysis of promoter regions in TSA-, TPX-, and ITSA1-responsive genes was next undertaken using recently developed *HumanUpstream* software (I.L., M.-C.J.K., O. Lipan, X. Zhou, K.-F.S., A.M. Bowcock, and W.H. Wong, unpublished data). Human orthologs of murine genes on the Affymetrix U74Av2 array were obtained using the Institute for Genomic Research (TIGR) TOGA database. For TSA-activated transcripts, 28 human ortholog promoter sequences were obtained (from a set of 111 total genes). Likewise, 28 sequences were identified for TPX-activated genes (70 total genes), 28 for ITSA1-activated genes (78 total genes), and 11 for ITSA1-repressed genes (24 total genes). Common frameworks of transcription factor binding sites were defined for each cluster of promoter sequences, and significant models within these subsets of the total data set identified (also see Supplemental Data at http://www.chembiol.com/cgi/content/full/10/5/397/DC1 or write to chembiol@cell.com for a PDF).

Promoter regions of TSA and TPX-upregulated genes were enriched in Sp1 sites, alone or in combination with other transcription factor binding sites. Sp1 sites are responsive to TSA [35] and TPX and are known to regulate expression of p21. Sp1 binding sites thus appear to be general HDAC-related regulatory elements. Analysis of the most highly upregulated transcript populations (TSA, >8-fold; TPX, >2-fold) provided evidence of specificity between promoters targeted by TSA and TPX. The E2F promoter was more generally associated with TSA-regulated transcripts, although it mediates the activity of TPX to a lesser extent. E2F represses transcription though association with class I HDAC1 [36]. The cAMP-response element binding proteins (CREB) pro-

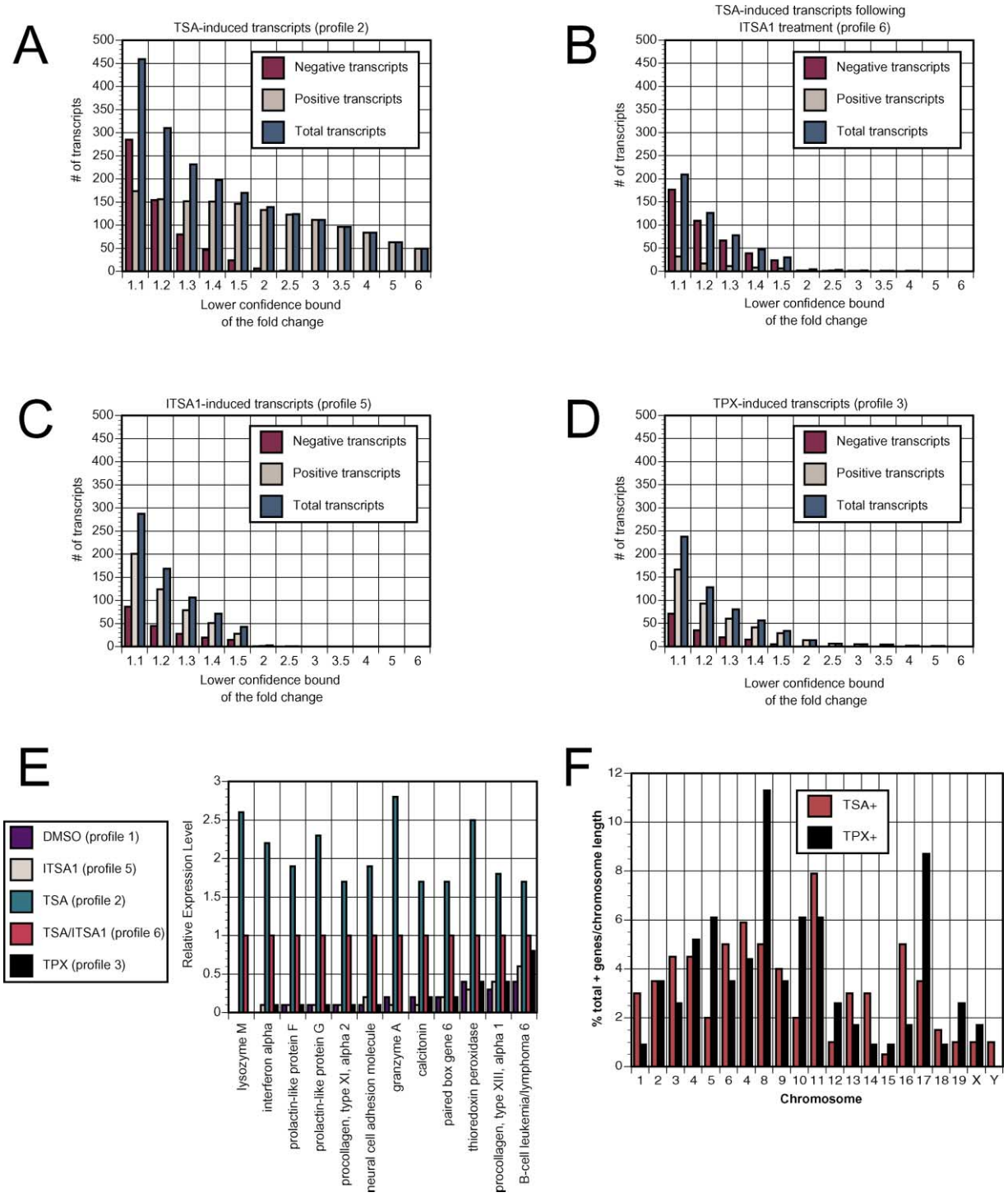

Figure 6. ITSA1 Suppresses TSA-Activated Transcription in Murine ES Cells

(A) TSA-induced transcripts (profile 2): number of transcripts as a function of fold-change.

(B) TSA-induced transcripts following treatment with ITSA1 (profile 6): number of transcripts as a function of fold-change.

(C) ITSA1-induced transcripts (profile 5): number of transcripts as a function of fold-change.

(D) TPX-induced transcripts (profile 3): number of transcripts as a function of fold-change.

(E) Relative expression levels of TSA-induced, ITSA1-suppressed transcripts with a previously reported relationship to HDACs or the cell cycle.

(F) Chromosomal mapping of TSA versus TPX upregulated genes normalized with respect to chromosome length.

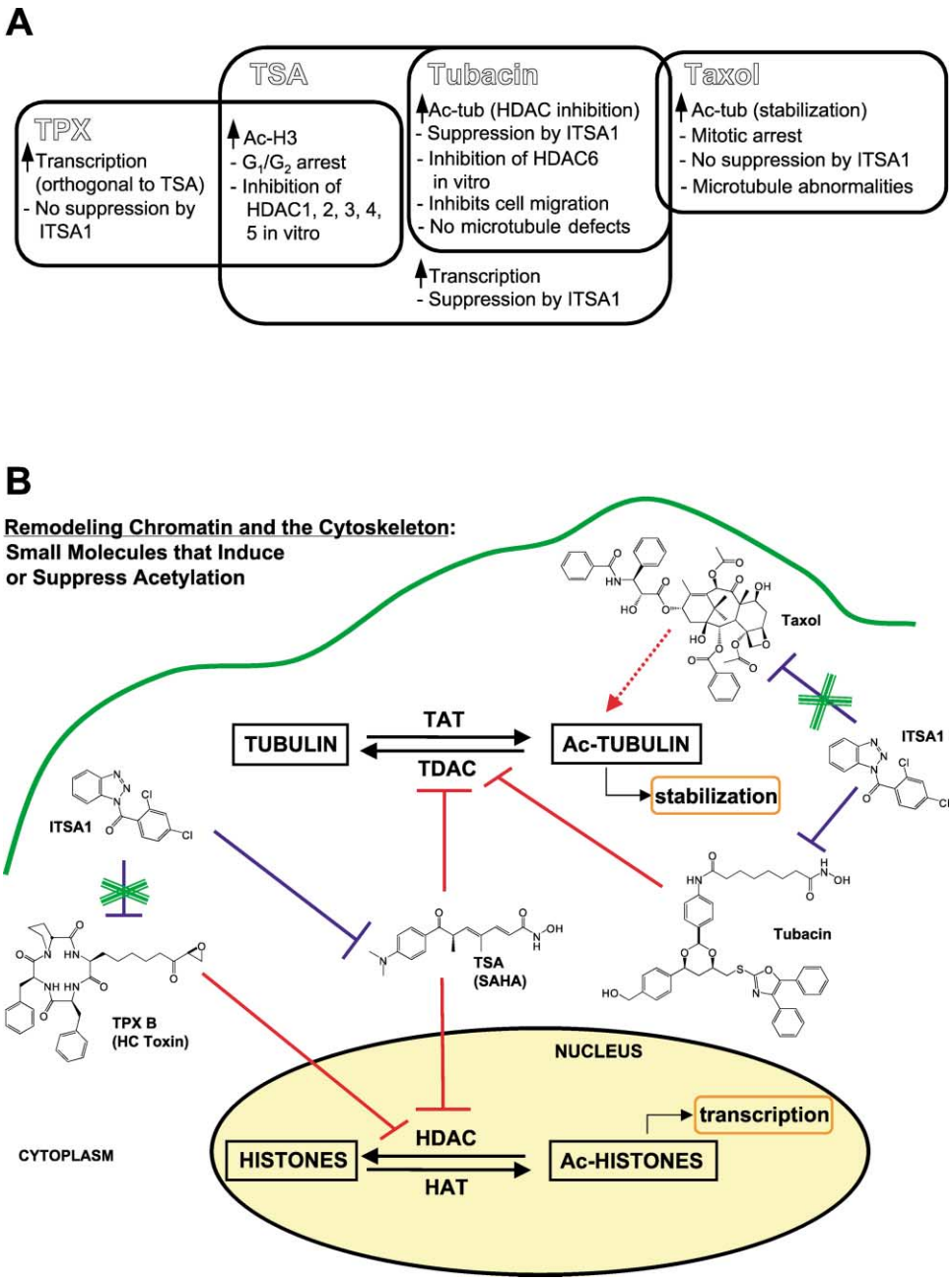

Figure 7. Molecular Tools for the Dissection of Cellular Acetylation-Related Processes

(A) Distinct and overlapping properties of small molecules that promote histone and/or tubulin acetylation in mammalian cells.

(B) An interaction map illustrating the known roles of histone and/or tubulin acetylation-inducing molecules in relation to TSA suppressor ITSA1.

moter was identified in combination with other promoters upstream of TSA-activated and ITSA1-suppressed genes. CREB may be relevant to ITSA1's suppression of TSA-induced histone acetylation, as the HAT activity of Creb binding protein (CBP) is associated with transcriptional activation. Myocyte enhancer factor 2 (MEF2) binding sites were over-represented in promoter regions of genes highly upregulated by TPX. MEF2-dependent transcription is repressed by class II HDACs like HDAC4 [37] and HDAC5. TPX also inhibits class I HDACs in cells, as the cDNA encoding HDAC1 was initially cloned following isolation of HDAC1 with a TPX-based affinity resin [38]. Promoter analysis thus provides evidence that TSA and TPX may act at certain functionally distinct sites within the genome, perhaps by selectively targeting different classes of HDACs.

Molecular Tools for the Dissection of Cellular Acetylation-Related Processes

Orthogonal and overlapping activities of four distinct small molecules that induce cellular histone and/or tubulin acetylation phenotypes are summarized in Figure

7A. Cellular activities associated with TSA, TPX, tubacin, and taxol have been analyzed and distinguished though ITSA1 suppression (Figure 7B). ITSAs represent new molecular probes of protein acetylation in cell cycle progression, transcriptional activation, and cytoskeletal stability. Although the direct target(s) of ITSA1 remains elusive, it likely is related to protein complexes associated with an acetylated state of chromatin. Further studies aimed at elucidating the target are currently ongoing. ITSAs may serve as tools to indicate differences between cell lines or tumors refractory to HDAC inhibition or exhibiting altered responses [39]. Moreover, tumors targeted by HDAC inhibitor therapy will likely develop resistance to these agents. Cellular resistance mechanisms could presumably resemble ITSA suppression, and identifying ITSA targets may shed light upon the adaptive resistance process. In addition, ITSAs may serve to sensitize cells to other chemotherapeutic drugs, since bypassing cell cycle checkpoints is known to contribute to genomic instability.

A substantial body of evidence has been amassed against a role for tubulin acetylation in TSA-induced cell cycle arrest. Consequently, tubulin acetylation represents an additional cellular consequence of treatment with hydroxamate-based HDAC inhibitors. In initial studies, the TDAC-selective inhibitor tubacin has been found to inhibit cell migration [23], an activity of therapeutic interest with respect to metastasis and angiogenesis. The overall clinical potential of molecules like SAHA and TSA may therefore be limited (or possibly enhanced) due to effects on the cytoskeleton. Nonetheless, acetylation of tubulin is a variable that should be considered in the ongoing clinical trials of hydroxamic acid-based HDAC inhibitors. Through cell-based screening, identification of TSA-like HDAC inhibitors that lack TDAC activity is also possible [22]. Natural products like TPX may appear to function globally in this manner, but disparate mechanisms of cell cycle arrest and transcriptional activation versus TSA have been observed.

Significance

Hydroxamate-based HDAC inhibitors related to trichostatin (TSA) are currently undergoing clinical trials for the treatment of cancer. These small molecules are generally believed to function by inducing cell cycle arrest or apoptosis in transformed cell lines. Discovery of new small molecules for use in analysis of TSA-induced cell cycle arrest has been accomplished though a cell-based suppressor screen. Trichostatin suppressors (ITSAs) represent valuable new tools for the study of acetylation-related phenotypes in mammalian cell lines. ITSAs suppress TSA-induced histone and tubulin acetylation, transcriptional activation, and cell cycle arrest, providing numerous avenues of study. Furthermore, ITSA analysis has elucidated nonoverlapping mechanisms resulting in histone hyperacetylation in the action of HDAC inhibitors TSA and TPX. Our experiments also suggest that TSA-induced tubulin acetylation has no bearing on cell cycle or transcriptional events. However, the consequences of tubulin acetylation on other cellular pathways should be considered as HDAC inhibitors are assessed in clinical cancer trials. Cell-based screening for chemical genetic modifiers of chromatin remodeling agents may contribute to the current understanding of gene expression and the cellular activities of small molecules employed as therapeutics. Chemical genetic modifier screens offer a powerful new approach to the discovery of small molecule probes.

Experimental Procedures

Materials

Trichostatin A, HC Toxin, nocodazole, 5′-bromo-2-deoxyuridine, paclitaxel (taxol), and camptothecin were from Sigma, Hoechst 33342 from Molecular Probes, and ITSA1, ITSA2, ITSA3, ITSA4, ITSA5, nITSA1-A, and nITSA1-B from Chembridge. Suberoylanilide hydroxamic acid was synthesized by Dr. Greg Copeland, and trapoxin B was synthesized by Dr. Jack Taunton. FK228 was obtained from Dr. Minoru Yoshida (University of Tokyo), and anti-TG-3 antibody was obtained from Dr. Peter Davies (Albert Einstein College of Medicine). Anti-BrdU and anti-PARP antibodies were from BD Biosciences Pharmingen, anti-acetylated α-tubulin (6-11B-1), anti-cyclin E, and anti-histone deacetylase 1 antibodies were from Sigma, anti-diacetyl-histone H3 antibody was from Upstate Biotechnology, anti-cdc2^{p34} and anti-cyclin A antibodies were from Santa Cruz Biotechnology, and anti-p21 antibody (Ab-5) was from Oncogene. Peroxidase-linked anti-rabbit and anti-mouse IgG antibodies were from Amersham Pharmacia Biotech, and Texas methyl red (TMR)-conjugated anti-mouse IgG antibody was from Molecular Probes.

Cell Culture

A549 cells (ATCC, human lung carcinoma) were maintained at 37°C with 5% CO_2 in Dulbecco's modified Eagle's medium (DMEM) supplemented with 10% fetal bovine serum (FBS), 100 units/ml penicillin G sodium, 100 μg/ml streptomycin sulfate (1% P/S), and 2 mM L-glutamine (1% L-Gln) (all from Gibco BRL). Murine FM3A and TR303 cells ([8]; from Dr. Minoru Yoshida, University of Tokyo) were maintained in RPMI 1640 medium at 37°C with 5% CO_2 supplemented with 10% FBS, 1% P/S, 1% L-Gln. Murine embryonic stem cells (Rosa 26.1; from Dr. Elizabeth Robertson, Harvard University) were maintained in DMEM supplemented with 15% defined fetal bovine serum (Hyclone), 1% P/S, 1% L-Gln, 100 μM nonessential amino acids (1%; Gibco BRL), 0.01 μl/ml β-mercaptoethanol (Sigma), 1 unit/ml leukemia inhibitory factor (LIF, Sigma).

TG-3 Cytoblot Assay

A549 cells were seeded in 40 μl DMEM$^+$ (4000 cells/well) in white 384-well plates (Nalge Nunc, tissue culture treated) using a liquid dispenser (Multidrop 384, Labsystems) and allowed to attach overnight at 37°C with 5% CO_2. TSA (5 μl, 3 μM [(final) = 300 nM TSA/well]) was added to each well and incubation continued (5 hr). Library compounds (9600 molecules, Diverse E set, Chembridge) dissolved in DMSO ($\sim$5 mg/ml) were then pin transferred (50–200 nl to each well, [final] = $\sim$20 μM compound/well) along with addition of nocodazole (5 μl, 3.2 μM, [final] = 332 nM nocodaazole/well). Following 16 hr incubation, the percentage of cells in mitosis was assayed using the TG-3 mAb as described [9]. Data were collected on an Analyst plate reader (LJL Biosystems) with 0.1 s integration time. After two rounds of screening, compounds that increased TG-3 reactivity by 2-fold or greater than control cells were considered "hits" (ITSAs).

BrdU Cytoblot Assay

Murine ES cells were seeded in 40 μl ES medium (4000 cells/well) in white 384-well plates (Nalge Nunc, tissue culture treated) using a liquid dispenser (Multidrop 384, Labsystems) and allowed to attach overnight at 37°C with 5% CO_2. TSA (5 μl, [final] = 78 nM–5 μM TSA/well) was added to each well, and plates were incubated 5 hr. ITSA1-4 (5 μl, [final] = 12.5–200 μM ITSA/well) or camptothecin (5 ml, [final] = 78 nM–5 μM camptothecin/well) were added and incubation was continued 16 hr. BrdU (10 μl, [final] = 10 μM BrdU/well) was added and incubation was continued 2 hr. Cells incorporating BrdU were detected using anti-BrdU Ab and ECL reagents

(Amersham Pharmacia) as described [9]. In a dark room, film (X-OMAT AR, Kodak Corporation) was placed on top of the plate for 1–5 min, then developed in a Kodak M35A X-OMAT processor.

Immunoblotting Experiments

Cells (A549 or murine ES) were seeded into 5 or 10 cm dishes, allowed to attach overnight, and small molecules were added as DMSO stock solutions. Following treatment, cells were harvested using trypsin/EDTA (Gibco BRL), washed with phosphate buffered saline (PBS; pH 7.4; 2 × 5 ml), and lysed at 4°C (30 min) in ELB^+ buffer (50 mM HEPES [pH 7], 250 mM NaCl, 5mM EDTA [pH 8], 0.1% NP-40) with a protease inhibitor cocktail (PIC, Boehringer-Mannheim). Proteins were separated by SDS-PAGE gel electrophoresis, transferred to PVDF membrane (Millipore), and incubated with antibodies diluted in PBST (PBS [pH 7.4], 0.1% Tween-20). Detection was accomplished using ECL reagents. When not shown, a nonspecific protein band was used to confirm protein normalization.

In Vitro Histone Deacetylase Assay

[^{3}H]acetate-incorporated histones were isolated from butyrate-treated HeLa cells as described [40]. HeLa cell pellets (National Cell Culture Facility) were lysed in JLB^+ (50 mM Tris [pH 8], 150 mM NaCl, 10% glycerol, 0.5% Triton X-100) supplemented with PIC. Lysates were treated with TSA and ITSA1 and incubated with [^{3}H]-acetylated histones for 2 hr at 37°C. HDAC activity was determined by scintillation counting of the ethyl acetate soluble [^{3}H]acetic acid as described [38, 40]. Each assay point was run in triplicate.

Immunofluorescence Microscopy

A549 cells were seeded onto glass coverslips at 80%–90% confluency, and compounds were added diluted in cellular medium. Following incubation at 37°C for 18 hr, cells were fixed (0.2% glutaraldehyde), permeabilized (50 mM K-Pipes [pH 6.8], 5 mM EGTA, 0.5 mM $MgCl_2$, 0.1% Triton X-100), and stained with an anti-acetylated-α-tubulin antibody (6-11B-1) and Hoechst 33342 dye diluted in antibody dilution buffer (ADB, Tris buffered saline (TBS), 0.1% Triton X-100, 2% bovine serum albumin, 0.1% sodium azide), followed by a secondary TMR-conjugated anti-mouse IgG antibody (Molecular Probes). Images were obtained using a Leitz microscope.

Cytotoxicity Assay

Exponentially growing cultures of FM3A and TR303 cells [8] were suspended at an initial density of $\sim 2 \times 10^5$ cells/ml in $RPMI^+$. After incubation with TSA (80 nM) or DMSO for variable times, viable cell numbers were determined in a hemacytometer using the trypan blue exclusion method. The Western blot experiment in Figure 4B was obtained after a 48 hr treatment period.

FACS Analysis

A549 cells (~75% confluent, 10 cm dishes) were treated with DMSO (0.1% v/v), TSA (500 nM), or HC Toxin (500 nM) for 4.5 hr, then with either DMSO (0.1% v/v) or ITSA1 (50 μM) for 17.5 hr. Samples were rinsed in PBS, trypsinized, fixed (2 hr, 70% ethanol, 30% PBS, 4°C), washed, and stored overnight in PBS (4°C). Samples were blocked 45 min in antibody dilution buffer (ADB = TBS, 0.1% Triton X-100, 2% bovine serum albumin, 0.1% sodium azide), aspirated, and incubated in ADB with mouse anti-acetylated tubulin IgG (6-11B-1, Sigma, 1:500 v/v, overnight, 4°C). Samples were washed and incubated in ADB with fluorescein isothiocyanate-conjugated goat anti-mouse IgG (Santa Cruz, 1:200 v/v, 1 hr, room temperature). Cells were washed twice in TBS, resuspended in ribonuclease A (100 μl, Sigma, 100 μg/ml), and incubated 5 min (37°C). To measure the DNA content, propidium iodide (PI; 400 μl, Molecular Probes, 50 μg/ml) was added and incubated 1 hr at room temperature. (Samples were processed as above, but only information derived from DNA content was necessary for this study.) Samples were analyzed using a FACScanII flow cytometer (Becton-Dickinson) at the Dana Farber Cancer Institute, exciting at 488 nm and measuring PI fluorescence though a 600 nm wavelength filter. Cell cycle distributions and apoptosis analysis were calculated from 10^4 cells and modeled using ModFit LT (V2.0) software.

Zebrafish Protocol

Homozygous transgenic zebrafish [26] were bred to wild-type zebrafish in synchronized pairwise crosses as described [41] to generate embryos that all expressed GFP. Eggs were collected and kept in embryo buffer [41] supplemented with 40 U penicillin G and 40 μg streptomycin. At 24 hr post-fertilization (hpf), embryos were treated with 0.003% 1-phenyl-2-thiourea (PTU) to inhibit melanin synthesis [41]. At 48 hpf, 10 fish were placed in a 6-well plate with 2 ml of PTU in embryo media. Stocks of valproic acid, TSA, ITSA1, nITSA1-A, and nITSA1-B were added directly to wells containing fish. Fish were grown at 28.5°C for an additional 48 hr prior to examination. At 96 hpf, treated fish were anesthetized with tricaine [41], viewed, and photographed under a Leica MZFLIII dissecting microscope (Leica Microsystems, Bannockburn, IL) using a GFP filter set.

Transcriptional Profiling

Profiling samples were prepared using Affymetrix protocols. Duplicate samples were independently prepared from different cultures of cells on different occasions. Murine ES cells (~10×10^7 cells, 10 cm dish, ~80% confluent) were treated with DMSO, TSA (300 nM), TPX (50 nM), or tubacin (2 μM) for 2 hr, then with DMSO or ITSA1 (50 μM) for 30 min. Cells were harvested and total RNA was isolated using an RNeasy kit (Qiagen), yielding ~150–250 μg/sample. Purification (Oligotex direct mRNA mini kit, Qiagen) then afforded ~1–4 μg poly A^+ mRNA/sample (1%–4% yield). $T7(dT)_{24}$ primer (Genset Oligos) was used for cDNA synthesis with the Superscript Choice System (Invitrogen) for first and second strand synthesis. Biotinylated probes were prepared using the BioArray High-Yield RNA Transcript Labeling Kit (Enzo Diagnostics), and fragmentation (35 min, 94°C) provided ~30-60 μg cRNA/sample. Fragmented cRNA (15 μg) was then submitted to the MIT Biopolymers Facility for hybridization to Affymetrix murine gene chip U74Av2. DChip1.0 software ([29], http://www.biostat.harvard.edu/complab/dchip/) was used for data analysis. Present calls ranged between 39%–49% for all 12 arrays analyzed. Following chip normalization and model-based expression processing, duplicate gene lists were pooled by a weighted averaging method. Samples were compared to DMSO control profile (1) at various levels of fold change, and the lower statistical bound of the observed fold change was used for analysis (see Supplemental Data at http://www.chembiol.com/cgi/content/full/10/5/397/DC1 or write to chembiol@cell.com for a PDF).

Promoter Analysis

To obtain the promoter sequence for each mouse gene in the clusters to be analyzed, the Institute for Genomic Research (TIGR) Orthologous Gene Alignment (TOGA, now EGO, Eukaryotic Gene Orthologs) database was used to generate pairwise comparisons between the tentative consensus sequences that comprise the TIGR Human and Mouse Gene Indices (I.L., M.-C.J.K., O. Lipan, X. Zhou, K.-F.S., A.M. Bowcock, and W.H. Wong, unpublished data). Tentative human consensus (THC) orthologs and their promoter sequences were identified for many of the selected mouse genes. To obtain a list of known transcription factor binding sites that occur in the same relative order in most sequences, FrameWorker of Genome Exploring and Modeling Software (GEMS, Genomatix) was employed to extract a common framework of binding sites from a set of DNA sequences. The framework model is sufficient to find the promoter but is not a complete description of all functional elements. A model derived from such results can be used to scan databases for additional sequences that show a similar functional organization even in the absence of direct sequence similarity. To evaluate the statistical significance of models found with FrameWorker, 200 control groups of sequences derived from the *HumanUpstream* database were randomly sampled, each containing the same number of sequences as the experimental group. These groups were analyzed with ModelInspector professional (GEMS, Genomatix) utilizing the previously found models to scan sequences for regulatory units matching the models. The program returns the numbers of matches for each model in each of 200 control groups. The mean, standard deviation, and Z score (observation minus mean divided by SD) were calculated for each model, and models with Z scores ≥ 3 were considered significant (see Supplemental Data at the URL above).

Acknowledgments

We thank Drs. Cheng Li and Wing H. Wong for providing dCHIP software and assistance in its use, Dr. Greg Copeland for the synthesis of SAHA, Dr. Chistina Grozinger for helpful discussions, and Dr. Carol Chang for assistance with database analysis. This research was supported by the National Institute of General Medical Sciences (GM-38627, awarded to S.L.S.). K.M.K. was supported by Damon Runyon Cancer Research Foundation Fellowship DRG-1650, I.L. by NSF grant DBI-0196176, J.C.W. by an NSF pre-doctoral fellowship, and M.-C.J.K. by a Howard Hughes pre-doctoral fellowship. S.L.S. is an Investigator at the Howard Hughes Medical Institute in the Department of Chemistry and Chemical Biology at Harvard University.

Received: January 24, 2003
Revised: March 27, 2003
Accepted: March 28, 2003
Published: May 16, 2003

References

1. Cress, W.C., and Seto, E. (2000). Histone deacetylases, transcriptional control, and cancer. J. Cell. Physiol. *184*, 1–16.
2. Marks, P.A., Rifkind, R.A., Richon, V.M., Breslow, R., Miller, T., and Kelly, W.K. (2001). Histone deacetylases and cancer: causes and therapies. Nat. Rev. Cancer *1*, 194–202.
3. He, L.-Z., Tolentino, T., Grayson, P., Zhong, S., Warrel, R.P., Jr., Rifkind, R.A., Marks, P.A., Richon, V.M., and Pandolfi, P.P. (2001). Histone deacetylase inhibitors induce remission in transgenic models of therapy-resistant acute promyelocytic leukemia. J. Clin. Invest. *108*, 1321–1330.
4. Piekarz, R.L., Robey, R., Sandor, V., Bakke, S., Wilson, W.H., Dahmoush, L., Kingma, D.M., Turner, M.L., Altemus, R., and Bates, S.E. (2001). Inhibitor of histone deacetylation, depsipeptide (FR901228), in the treatment of peripheral and cutaneous T-cell lymphoma: a case report. Blood *98*, 2865–2868.
5. Hughes, R.E. (2002). Polyglutamine disease: acetyltransferase awry. Curr. Biol. *12*, R141–R143.
6. Williams, R.S.B., Cheng, L., Mudge, A.W., and Harwood, A.J. (2002). A common mechanism of action for thee mood-stabilizing drugs. Nature *417*, 292–295.
7. Grozinger, C.M., and Schreiber, S.L. (2002). Deacetylase enzymes: biological functions and the use of small-molecule inhibitors. Chem. Biol. *9*, 3–16.
8. Yoshida, M., Kijama, M., Akita, M., and Beppu, T. (1990). Potent and specific inhibition of mammalian histone deacetylase both *in vivo* and *in vitro* by trichostatin A. J. Biol. Chem. *265*, 17174–17179.
9. Stockwell, B.R., Haggarty, S.J., and Schreiber, S.L. (1999). High-throughput screening of small molecules in miniaturized mammalian cell-based assays involving post-translational modifications. Chem. Biol. *6*, 71–83.
10. Haggarty, S.J., Mayer, T.U., Miyamoto, D.T., Fathi, R., King, R.W., Mitchison, T.J., and Schreiber, S.L. (2000). Dissecting cellular processes using small molecules: identification of colchicine-like, taxol-like, and other small molecules that perturb mitosis. Chem. Biol. *7*, 275–286.
11. Richon, V.M., Emiliani, S., Verdin, E., Webb, Y., Breslow, R., Rifkind, R.A., and Marks, P.A. (1998). A class of hybrid polar inducers of transformed cell differentiation inhibits histone deacetylases. Proc. Natl. Acad. Sci. USA *95*, 3003–3007.
12. Kim, Y.B., Ki, S.W., Yoshida, M., and Horinouchi, S. (2000). Mechanism of cell cycle arrest caused by histone deacetylase inhibitors in human carcinoma cells. J. Antibiot. (Tokyo) *53*, 1191–1200.
13. Schreiber, S.L., and Bernstein, B.E. (2002). Signaling network model of chromatin. Cell *111*, 771–778.
14. Kijima, M., Yoshida, M., Sugita, K., Horinouchi, S., and Beppu, T. (1993). Trapoxin, an antitumor cyclic tetrapeptide, is an irreversible inhibitor of mammalian histone deacetylase. J. Biol. Chem. *268*, 22429–22435.
15. Nakajima, H., Kim, Y.B., Terano, H., Yoshida, M., and Horinouchi, S. (1998). FR901228, a potent antitumor antibiotic, is a novel histone deacetylase inhibitor. Exp. Cell Res. *241*, 126–133.
16. Furumai, R., Komatsu, Y., Nishino, N., Khochbin, S., Yoshida, M., and Horinouchi, S. (2001). Potent histone deacetylase inhibitors built from trichostatin A and cyclic tetrapeptide antibiotics including trapoxin. Proc. Natl. Acad. Sci. USA *98*, 87–92.
17. Guardiola, A.R., and Yao, T.-P. (2002). Molecular cloning and characterization of a novel histone deacetylase HDAC10. J. Biol. Chem. *277*, 3350–3356.
18. Furumai, R., Matsuyama, A., Kobashi, N., Lee, K.H., Nishiyama, M., Nakajima, H., Tanaka, A., Komatsu, Y., Nishino, N., Yoshida, M., et al. (2002). FK228 (depsipeptide) as a natural prodrug that inhibits class I histone deacetylases. Cancer Res. *62*, 4916–4921.
19. Piperno, G., LeDizet, M., and Chang, X.-j. (1987). Microtubules containing acetylated α-tubulin in mammalian cells in culture. J. Cell Biol. *104*, 289–302.
20. Hubbert, C., Guardiola, A., Shao, R., Kawaguchi, Y., Ito, A., Nixon, A., Yoshida, M., Wang, X.-F., and Yao, T.-P. (2002). HDAC6 is a microtubule-associated deacetylase. Nature *417*, 455–458.
21. Haggarty, S.J., Koeller, K.M., Wong, J.C., Butcher, R.A., and Schreiber, S.L. (2003). Multidimensional chemical genetic analysis of diversity-oriented synthesis-derived deacetylase inhibitors using cell-based assays. Chem. Biol., this issue, 383–396.
22. Sternson, S.M., Wong, J.C., Grozinger, C.M., and Schreiber, S.L. (2001). Synthesis of 7200 small molecules based on a substructural analysis of the histone deacetylase inhibitors trichostatin and trapoxin. Org. Lett. *3*, 4239–4242.
23. Haggarty, S.J., Koeller, K.M., Wong, J.C., Grozinger, C.M., and Schreiber, S.L. (2003). Domain-selective small-molecule inhibitor of histone deacetylase 6 (HDAC6)-mediated tubulin deacetylation. Proc. Natl. Acad. Sci. USA *100*, 4389–4394.
24. Peterson, R.T., Link, B.A., Dowling, J.E., and Schreiber, S.L. (2000). Small molecule developmental screens reveal the logic and timing of vertebrate development. Proc. Natl. Acad. Sci. USA *97*, 12965–12969.
25. Hyatt, G.A., Schmitt, E.A., Fadool, J.M., and Dowling, J.E. (1996). Retinoic acid alters photoreceptor development in vivo. Proc. Natl. Acad. Sci. USA *93*, 13298–13303.
26. Perkins, B.D., Kainz, P.M., O'Malley, D.M., and Dowling, J.E. (2002). Transgenic expression of a GFP-rhodopsin COOH-terminal fusion protein in zebrafish rod photoreceptors. Vis. Neurosci. *19*, 257–264.
27. Bernstein, B.E., Tong, T.K., and Schreiber, S.L. (2000). Genomewide studies of histone deacetylase function in yeast. Proc. Natl. Acad. Sci. USA *97*, 13708–13713.
28. Mariadson, J.M., Corner, G.A., and Augenlicht, L.H. (2000). Genetic reprogramming in pathways of colonic cell maturation induced by short chain fatty acids: comparison with trichostatin A, sulindac, and curcumin and implications for chemoprevention of colon cancer. Cancer Res. *60*, 4561–4572.
29. Li, C., and Wong, W.H. (2001). Model-based analysis of oligonucleotide arrays: expression index computation and outlier detection. Proc. Natl. Acad. Sci. USA *98*, 31–36.
30. Diamond, S.E., and Gutierrez-Hartmann, A. (2000). The pit-1β domain dictates active repression and alteration of histone acetylation of the proximal prolactin promoter. J. Biol. Chem. *275*, 30977–30986.
31. Ammerpohl, O., Schmitz, A., Steinmiller, L., and Renkawitz, R. (1998). Repression of the mouse M-lysozyme gene involves both hindrance of enhancer factor binding to the methylated enhancer and histone deacetylation. Nucleic Acids Res. *26*, 5256–5260.
32. Fan, Z., Beresford, P.J., Zhang, D., Xu, Z., Novina, C.D., Yoshida, A., Pommier, Y., and Lieberman, J. (2003). Cleaving the oxidative repair protein Ape1 enhances cell death mediated by granzyme A. Nat. Immunol. *4*, 145–153.
33. Ramalho-Santos, M., Yoon, S., Matsuzaki, Y., Mulligan, R.C., and Melton, D.A. (2002). "Stemness": transcriptional profiling of embryonic and adult stem cells. Science *298*, 597–600.
34. Webb, Y., Zhou, X., Ngo, L., Cornish, V., Stahl, J., Erdjument-Bromage, H., Tempst, P., Rifkind, R.A., Marks, P.A., Breslow, R., et al. (1999). Photoaffinity labeling and mass spectrometry

identify ribosomal protein S3 as a potential target for hybrid polar cytodifferentiation agents. J. Biol. Chem. *274*, 14280–14287.

35. Sowa, Y., Orita, T., Minamikawa, S., Nakano, K., Mizuno, T., Nomura, H., and Sakai, T. (1997). Histone deacetylase inhibitor activates the WAF1/Cip1 gene promoter though the Sp1 sites. Biochem. Biophys. Res. Commun. *241*, 142–150.
36. Brehm, A., Miska, E.A., McCance, D.J., Reid, J.L., Bannister, A.J., and Kouzarides, T. (1998). Retinoblastoma protein recruits histone deacetylase to repress transcription. Nature *391*, 597–601.
37. Miska, E.A., Karlsson, C., Langley, E., Nielsen, S.J., Pines, J., and Kouzarides, T. (1999). HDAC4 deacetylase associates with and represses the MEF2 transcription factor. EMBO J. *18*, 5099–5107.
38. Taunton, J., Hassig, C.A., and Schreiber, S.L. (1996). A mammalian histone deacetylase related to the yeast transcriptional regulator Rpd3. Science *272*, 408–411.
39. Qiu, L., Burgess, A., Fairlie, D.P., Leonard, H., Parsons, P.G., and Gabrielli, B.G. (2000). Histone deacetylase inhibitors trigger a G2 checkpoint in normal cells that is defective in tumor cells. Mol. Biol. Cell *11*, 2069–2083.
40. Hassig, C.A., Tong, J.K., Fleischer, T.C., Owa, T., Grable, P.G., Ayer, D.E., and Schreiber, S.L. (1998). A role for histone deacetylase activity in HDAC1-mediated transcriptional repression. Proc. Natl. Acad. Sci. USA *95*, 3519–3524.
41. Westerfeld, M. (1995). The Zebrafish Book, Third Edition (Eugene, OR: University of Oregon Press).